AD715751

A FRACTOGRAPHIC STUDY OF THE FATIGUE FAILURE OF AIRCRAFT WHEELS

BY

W. WIEBE

NATIONAL AERONAUTICAL ESTABLISHMENT

OTTAWA

NOVEMBER 1970

A FRACTOGRAPHIC STUDY OF THE FATIGUE FAILURE OF AIRCRAFT WHEELS

by

W. Wiebe

A. H. Hall, Head
Structures & Materials Laboratory

F. R. Thurston
Director

SUMMARY

A survey of aircraft wheel failures, and a review of the parameters involved in the qualification tests for aircraft wheels, have indicated a need for accurate information concerning wheel service loading conditions in order to formulate realistic wheel fatigue test spectra. The fractographic examination of three types of wheels from modern aircraft has emphasized the significance of corrosion in the nucleation of fatigue cracks, and has indicated that landing impact loads and brake applications at high speeds may contribute to the growth of the cracks.

Several types of macroscopic growth "bands" or "lines" that are frequently observed on the fatigue fracture surfaces of laboratory specimens and of components that have failed in service, have been cited and described. Those lines observed on the fracture surfaces of the failed wheels were correlated with crack growth during aircraft "landing cycles". The derivation of fatigue crack growth rate information from these lines has facilitated the revision of wheel inspection schedules with the purpose of preventing the catastrophic failure of aircraft wheels.

TABLE OF CONTENTS

TABLES

ILLUSTRATIONS

A FRACTOGRAPHIC STUDY OF THE FATIGUE FAILURE OF AIRCRAFT WHEELS

1.0 INTRODUCTION

It is difficult to arrive at an accurate estimate of the number of catastrophic wheel failures that occur on modern aircraft, or of the number of aircraft wheels that are discarded because excessively long fatigue cracks have been detected in the wheel hubs. A recent survey[1] of thirteen major world airlines in which eight were able to provide information, indicated a total of some 216 main landing gear aluminum alloy wheel failures on one common type of commercial jet transport. Although it was not possible to ascertain the exact period of service covered by this survey, it is estimated that it would have covered a period, not in excess of ten years. One of the airlines was able to provide extremely detailed service information on 26 failed wheels, thereby presenting an informative sampling of wheel service history for this type of aircraft. The failures recorded over a period of approximately ten years, indicated an average service life of 5.5 years for the failed wheels, with an average endurance of 19,000 roll miles. The endurances ranged from 1,835 to 39,000 roll miles. Failures occurred in both inboard and outboard halves of the wheels, and in most instances were attributed to fatigue. Corrosion was listed as a probable cause of failure in five instances. The endurance ratio of 20 to 1 in roll miles to failure, suggests that in addition to the number of roll miles, other factors probably contributed significantly to the fatigue failure of the aircraft wheels. It is in part, the purpose of this paper to determine, with the aid of fractography, the nature of some of these parameters, and how they may affect the life of the wheels.

There is an apparent dearth of information concerning well-tailored, realistic fatigue qualification tests for aircraft

wheels. This probably stems, in part, from the fact that wheels are generally not considered to fall within the category of primary aircraft structure. This is understandable when it is considered that catastrophic failure of a single wheel on a dual or multiple-wheel undercarriage assembly does not, as a rule, pose a threat to the safety of the passengers, crew, or the aircraft as a whole. However, incidents of damage to jet engine nacelles by flying pieces of metal from shattered wheels, instances of fatal injury to ground personnel in the vicinity of the aircraft when catastrophic wheel failure occurred, and ingestion of rubber from concurrent tire failures, into rear-mounted jet engines, have proven to be costly and highly undesirable. In addition, down-time of the aircraft as a result of wheel failure, particularly if failure occurs at an airport without ready repair facilities, - not to mention the cost of replacement wheels and tires, all represent expense to the airline operator. Therefore it seems prudent to examine the circumstances surrounding wheel failures somewhat more closely in order to determine if prescribed wheel qualification tests for modern aircraft are adequately representative of service conditions.

Available information suggests that current fatigue qualification tests for aircraft wheels consist essentially of roll tests under maximum static load. The minimum requirements, stipulated for the "Roll Test" in the Aerospace Standard[2] for "Wheels and Brakes for Civil Aircraft Applications" state: "Wheel with tire installed shall withstand, without failure or development of cracks a roll life specified, under a load not less than the maximum static rating of the wheel". The specified roll distance is 1000 miles. The requirements appear to be somewhat flexible in that they further stipulate that where a longer service life is required, a roll test of greater duration

may be undertaken, and the exact conditions of test would be determined by agreement between the aircraft and wheel manufacturers. No apparent consideration has been given to the adverse effects of such parameters as landing impact loads, stresses in the wheel hubs due to brake application, landing side loads, and excess tire pressure to name a few. Behr and Campbell (1965)[3] state categorically that "Currently, no satisfactory method is available for evaluating the influence of metallurgical and environmental factors on the roll life of aircraft wheels. Service experience cannot be used effectively because necessary associated information is incomplete or non-existent".

Other specifications (1967)[4] require a complete static and dynamic analysis of wheel loads from which a loading spectrum is to be prepared. A complete stress analysis for all fatigue and static loads on all major components of the test wheel or wheel-brake assembly is also required. However, the required "roll test", which is intended to be an "index of the anticipated service fatigue life of the wheel", consists of a series of landings, or a continuous roll of the tire and wheel assembly against a rotating flywheel. No reference is made to the loading spectrum culminating from the dynamic analysis referred to earlier. The minimum requirements are stipulated as 1,500 miles at a load not less than that encountered on the aircraft at maximum taxi gross weight.

More recently (1968)[5] efforts appear to have been directed towards the establishment of more realistic wheel test load spectra by instrumentation of a Comet undercarriage in order to determine the nature of wheel, axle and undercarriage stresses generated by the limits of ground manoeuvring. The examination of failed aircraft wheels in this laboratory

substantiates the need for more realistic test load spectra for aircraft wheels, in that the fractographic findings have demonstrated that substantial fatigue damage may result from landing impact stresses and brake application. To date, parameters such as these have not been adequately catered for under the conventional "roll test" qualification requirements.

Modern jet airliners, having ground speeds of up to 250 miles per hour[5] are subjected to severe dynamic loads on landing. The tires absorb much of the landing impact energy. With tire inflation pressures ranging from 150 to 200 lb./in.^{2}, and tire deflections as high as 32 to 35 percent, due to landing impact, fatigue failures of aircraft wheel hubs in or adjacent to the tire bead seat radius appear to reflect the repeated outward flange bending loads that result from these high tire deflections. This view is substantiated to a considerable extent by fractographic studies of aircraft wheels that have failed in service. Here, macroscopic growth bands, on the fracture surfaces, frequently exhibit areas of ductile dimples amid regions of conventional fatigue striations when viewed in the electron microscope. Although the striations may be associated with cyclic stresses originating from wheel rotation, it is believed that the ductile dimples indicate short bursts of rapid crack growth corresponding to landing impact loads.

Another critical parameter to be considered in the endurance of aircraft wheels is the tire inflation pressure. Available information[1] suggests that on one common commercial jet transport the estimated wheel endurance falls from 40,000 to 10,000 roll miles when the tire inflation pressure is increased from 170 lb./in.^{2} to 190 lb./in.^{2}

Perhaps one of the more critical factors in the service failures of aircraft wheels is the initiation of the fatigue crack. Experience in this laboratory, in the course of the

fractographic examination of a number of aircraft wheels from several types of military and civil aircraft, indicates that in many instances corrosion plays a significant role in the initiation and early growth stages of fatigue cracks in the wheels. In some instances a well-defined corrosion pit can unequivocally be cited as the stress-raiser responsible for the initiation of the fatigue crack. When a corrosion pit is not so well defined, a small lightly discoloured semi-circular area on the fracture surface, apparently associated with corrosion, frequently defines the region of crack initiation. Current activities by some aircraft operators, aimed at minimizing the formation of corrosion pits on aircraft wheels involve the investigation of the effectiveness of new types of protective paints. In one instance, tests involving shot peening of the wheels after paint stripping are being conducted in an attempt to extend the life of the wheels by inducing compressive surface stresses. Information concerning the effect on the life extension of the wheels as a result of such treatments is not, as yet, available.

Meanwhile, aircraft operators appear to be increasing the frequency of their visual, ultrasonic, and eddy current inspection procedures of the wheels, as the service life of the wheels increases. In spite of these safeguards, incidents of catastrophic wheel failures are still being reported, because some fatigue cracks are not being detected in the early stages of their development. Under these circumstances this laboratory was requested to undertake a programme of fractographic analysis of several types of failed aircraft wheels, in an attempt to obtain information concerning fatigue crack propagation rates, thereby to aid in the establishment of acceptable wheel inspection schedules. The fractographic analysis involved the microscopic examination of the fracture surface

topography of three types of aircraft wheels that had failed in service. It consisted essentially of deriving counts of the crack progression "lines" or "bands" believed to be associated with crack growth during aircraft "landing and take-off" sequences or "cycles". The results indicated that crack growth rates, in terms of "number of landings" varied for different types of wheels, - and where catastrophic wheel failure had occurred, a marked increase in crack growth per landing was generally evident in the later stages of crack development.

2.0 FRACTOGRAPHIC FEATURES OF FATIGUE FAILURES RESULTING FROM REPETITIVE SEQUENTIAL LOADING

Before dealing with the quantitative fractographic analysis of the individual wheels, it might be advantageous to consider the microscopic fracture surface features of the various types of macroscopic growth bands, and how they can be utilized to educe quantitative information concerning fatigue crack growth rates. These bands are frequently encountered on the fracture surfaces of laboratory fatigue specimens and components failed in service, that have been subjected to repetitive sequential loading. Examination of the band topography in the electron microscope indicates that the history of the sequential load spectrum is frequently clearly defined on the fracture surface. Thus the microscopic content of the macroscopic bands permits accurate interpretation of their significance in terms of cyclic loading history. Although it is not always clear precisely why the macroscopic crack growth bands are visible, they have been known to represent slight alternate changes in the plane of crack propagation due to abrupt changes in load level. In other instances, a periodic repetition of bright and dull bands has been shown to represent alternate changes from the conventional fatigue mechanism (which is frequently accompanied by fatigue striation formation) to a rapid fracture mode accompanied by microvoid coalescence.

2.1 Fracture Surface Topography of Bands Formed in Laboratory Specimens

Two examples of laboratory fatigue specimens that have been subjected to repetitive load spectra, serve to illustrate the appearance of crack growth bands formed on the fracture surface of an aluminum alloy, and a steel specimen, and demonstrate how fatigue crack growth rates can be obtained from counts and spacing measurements of the bands.

2.1.1 Aluminum Alloy Spar of a Light Transport Aircraft.

Figure 1(a) illustrates the banded structure of the fracture surface typical of macroscopic topography formed in the fatigue failure of an aluminum alloy main spar web of the wing of a single engine aircraft. The wing, fatigue tested in the laboratory, was subjected to the load spectrum illustrated graphically in Figure 1(b). Each band was formed during the application of one load block, and represented some 20 equivalent hours of aircraft flying time.

The electron micrograph, Figure 2, illustrates at relatively high magnification the fracture surface topography of one macroscopic band. The variation in fatigue striation spacing with changes in cyclic load levels is clearly evident, and follows the cyclic loading sequence shown in Figure 1(b). The three lower load levels of the sequence did not produce fatigue striations, but formed a cleavage-like band at either end of the 20-hour spectrum. Thus the distance between the centres of the cleavage-like bands represents a single macroscopically visible band corresponding to a crack growth of some 35 microns during the application of one load block. A quantitative determination of fatigue crack growth rates in the spar, which involved counts of the bands on the various crack segments, has been reported in Reference 6.

2.1.2 Steel Bolt Fatigue Specimen

Although it is not possible to generalize on the nature

and the fracture mechanisms involved in the formation of the macroscopic crack growth lines on a fracture surface, they can nevertheless frequently be useful in determining the relationship between the periods of crack initiation and crack propagation in laboratory fatigue specimens. Assuming that it has been appropriately established that a given shift in mean load, (without change in the cyclic load amplitude), does not affect the fatigue life of a specimen to a significant degree, such a repetitive shift may produce macroscopic crack growth bands on the fracture surface that are amenable to counting and spacing measurements. In this manner, a fairly accurate crack growth rate history can be elicited, and variations in total specimen endurance can be ascribed to variations in crack initiation periods, or variations in crack propagation rates from specimen to specimen, whatever the case may be.

An example of this type of crack growth band on the fracture surface of a steel bolt is illustrated in Figure 3(a), and the repetitive loading sequence is sketched in Figure 3(b). The programme was such that the peak to peak tensile load amplitude remained constant at 15,000 lb. throughout the test, while the minimum and maximum loads shifted from 10,000 to 25,000 lb. to 20,000 and 35,000 lb. respectively. The 1,012 cycles per load block were divided approximately equally between the two load levels.

It is believed that the macroscopic bands observed on the fracture surface are initiated at that point in the programme where the load rises from 10,000 to 35,000 lb., or where it drops from 35,000 to 10,000 lb., - and are considered to be due to the effect on subsequent crack growth rate, of sudden changes in load level in an otherwise uniform cyclic load programme. The phenomenon has been ascribed to the process of crack tip blunting in the case of an increasing load, and resharpening of the crack tip by reversed plastic flow when the load is suddenly decreased.[7]

A further detailed treatment of the effect of mixed loads, and of the order of application of stress on fatigue damage is given by Forsyth in Reference 8.

In the earlier stages of fatigue crack growth the nature of the fracture surface topography was somewhat obscure. Because of the relatively low net section stresses, the bands on the fracture surface of the bolt were poorly defined, and their spacing was extremely fine. Therefore it was difficult to arrive at a firm conclusion regarding the fracture mechanisms involved in the formation of the banded structure. However, fractographic examination of the wider bands in the later stages of the fatigue crack growth (under conditions of increased net section stresses), indicated that the bright bands (Figure 3(a)) were formed by the mechanism of fatigue, as evidenced by the fatigue striations illustrated in Figure 4.

The dull bands were formed by the mechanism of localized ductile rupture, as indicated by the evidence of microvoid coalescence in the electron micrograph, Figure 5. This leads to the conclusion that as a result of the sudden change in cyclic load level, a momentary stress state approaching the ultimate stress level of the steel, must have existed at the tip of the crack. Presumably, this resulted in rapid crack growth over the width of the dull band during the short transient period of load level change, with subsequent reversion to the fatigue mechanism upon re-establishment of the steady state condition of cyclic loading.

The plot of crack length as a function of the number of load cycles shown in Figure 6, based on band counts and spacing measurements, provides a graphic illustration of the fatigue crack propagation history. Over the initial 0.1 mm. of crack penetration the growth history, involving some 150,000 load cycles is somewhat obscure due to the lack of definition of the fracture surface topography, - even at the higher levels

of magnification of the electron microscope. Extrapolation of the curve, however, suggests that crack penetration at 50,000 cycles was probably not in excess of 0.015 mm.

2.2 Fracture Surface Topography of Bands Formed in Service Fatigue Failures.

When comparing the macroscopic aspects of the fracture surface topography of service fatigue failures with those observed on laboratory fatigue specimens, one of the most striking differences is the random spacing of the bands or "macroscopic striations" on the fracture surfaces of the service failures. The low magnification light micrographs, Figures 7(a) and (b), illustrate and permit comparison of the appearance of the fracture surfaces of small fatigue cracks formed during a laboratory fatigue test, and in service, respectively, in the aluminum alloy spar caps of a single engine jet trainer. Whereas, the laboratory specimen exhibits more or less regularly spaced bands that correspond to the load blocks in the repetitive sequential cyclic loading programme, the macroscopic striations on the fracture surface of the service crack reflect the randomness in the magnitude of service loads experienced by the spar during flight manoeuvres and gusts.

2.2.1 Helicopter Rotor Blade Cuff Assembly

The fracture surface of a failed tine of an aluminum alloy main rotor-blade cuff assembly from a helicopter, illustrated in Figure 8(a) exhibits clearly defined macroscopic growth lines. Fractographic examination of the narrow bright bands indicated the presence of microscopic fatigue striations, Figure 8(b). As was the case in the laboratory steel bolt specimen (Section 2.1.2), fractographs of the wider dull bands (Figure 8(c)) indicated that crack growth had occurred by the mechanism of localized ductile rupture. This presumably occurred during high level load transients experienced in certain flight manoeuvres, and was followed by the reversion to the fatigue mechanism of crack growth with return to relatively steady state flight conditions, as evidenced by the numerous bright bands.

In order to make a meaningful estimate of crack growth rates from the analysis of the fracture surface topography in service failures of this type, some knowledge of dynamic strain or load magnitudes and sequences is essential, and it must be possible to correlate this information with the fracture surface topography. Since such information was not available in this instance, no attempt was made to obtain crack growth rate information.

3.0 THE FRACTOGRAPHIC ANALYSIS OF AIRCRAFT WHEELS

The fractographic analysis of three types of aluminum alloy failed main wheel hubs was undertaken in order to:

(i) Assess the nature of crack initiation and fracture mechanisms involved in the failures,

(ii) Determine the rates of crack propagation in order to facilitate revision of wheel inspection schedules, where necessary, to avoid the occurrence of catastrophic wheel failures.

The results of the fractographic examinations illustrated the variation in fatigue crack propagation rates in the different types of aircraft wheels examined. The studies of the micro-mechanisms of fracture operative during the formation of the macroscopic crack progression lines or "bands" indicated that landing impact loads and ground manoeuvres appear to contribute significantly to fatigue damage in aircraft wheels.

3.1 Fatigue Crack Initiation

Examination of the various wheel hubs that were submitted for fractographic analysis, frequently indicated some evidence of corrosion at or near the point of crack initiation. The fracture surfaces from the cracked type "A" wheel and the failed type "B" wheel, Figures 9 and 10 respectively, exhibited fairly well-defined corrosion pits at the sites of crack nucleation. An enlarged view of the pit in the type "A" wheel is given in Figure 11. The micrograph of a polished and etched section through the pit (Figure 12) clearly illustrates that corrosion has played a significant part in the nucleation of the

fatigue crack. In another instance a clearly defined pit was not in evidence, but a small semi-circular area of discolouration, Figure 13, believed to be associated with corrosion, was observed on the fracture surface of a failed type "B" wheel. For purposes of comparison, Figure 14 shows a number of small fatigue cracks that were nucleated from corrosion pits in the bead seat radius of an aluminum alloy main landing gear wheel of a jet trainer. The fracture surface of a cracked type "C" main landing gear wheel, Figure 15, exhibited no distinct evidence of corrosion, but the point of fatigue crack nucleation corresponded to a radial ridge across the thickness of the flange.

3.2 Crack Progression Lines

Curved macroscopic fatigue crack progression lines or "bands" emanating from the point of crack nucleation can readily be resolved on the wheel fracture surface illustrated in Figure 15. Since the validity of the following quantitative crack propagation analyses rests upon the proper interpretation of the nature of these bands in terms of the micro-mechanisms of fracture, a closer examination of the microscopic topographical features is warranted, and an attempt will be made to correlate them with certain aspects of the "landing, take-off" sequence, or "landing cycle" of the aircraft.

3.2.1 Aircraft "Landing Cycle"

The "landing cycle" of a typical jet transport could probably best be thought of as the sum total of roll miles and manoeuvres of the aircraft while on the ground, from time of engine start at the terminal ramp to engine shut down at the succeeding ramp. It is estimated that the average ground distance covered by the aircraft during one "landing cycle" would be of the order of 5 miles. An average ground sequence would probably include the following:

(i) Engine start at ramp
Push-back of aircraft, 150 ft.

(ii) Taxi to end of runway
Brakes and thrust reversal, as required.

(iii) Take-off roll, 0 to 170 mph, 5,000 ft.

(iv) Landing, 4,000 ft. roll.

(a) Touchdown of main wheels, at 1000 ft. down runway, 180 mph.

(b) Nose-wheel touchdown at 1200 ft., 2 second brake application, reducing speed to 100 to 115 mph.

(c) Two-engine thrust reversal to reduce speed to 70 mph., no brake application between speed interval 115 to 70 mph.

(d) 70 mph. and below, brakes as required.

(v) Taxi to ramp, 25 to 30 mph.
- some four brake applications, and 3 or 4 turns are estimated for each taxi to or from the ramp.

3.2.2 Interpretation of the Microscopic Aspects of Crack Progression Line Topography

An imprint of typical fatigue crack progression lines observed on the plastic replica of the fracture surface of the aluminum alloy type "C" wheel is shown at relatively low magnification in the transmitted light micrograph, Figure 16. The crack advance per line in the 1.0 mm. of crack length illustrated here ranges from 30 to 65 microns. The histogram, Figure 17, illustrates the line spacing distribution over the half crack-length interval 4 to 36 mm. The average line spacing, based on 329 measurements over the interval, was of the order of 41 microns. If it is assumed that macroscopic line spacings are proportional to the magnitude of the repeatedly applied stresses, as was shown to be the case for the spacings of microscopic striations, Figure 2, the distribution of line spacings indicated by the histogram probably reflects, in part, the variation in aircraft landing impact loads.

Near the crack origin, in the early stages of crack growth, the microscopic fracture surface topography of the various failed wheels appears in the form of "cleavage-like" bands, Figure 18. The lines or ridges running parallel to the direction of crack growth resemble the "river patterns" on cleavage fracture surfaces, but it is more likely that they are tear-ridges formed in a manner similar to those seen on conventional fatigue fracture surfaces with well-formed fine striations. Here the ridges were formed as the fatigue crack advanced simultaneously on several levels, (small arrows, Figure 2). Because of the relatively low net section cyclic stress conditions in the early stages of crack growth, the fine fatigue striations, if present, are probably not resolvable on the bands shown in Figure 18. The lines running perpendicular to the direction of crack growth represent successive positions of the crack front, and in the case of the failed aircraft wheels, their spacings are believed to represent the crack growth per "landing cycle".

The fracture surface topography of the type "C" wheel, illustrated in the electron micrograph of Figure 19, shows bands (interspersed with areas of fine striations) that, on the basis of a sampling of band spacing measurements, are believed to correspond to the macroscopic crack growth lines shown in Figure 16. The poor definition of the fine striations over the length of the fracture surface suggests corrosion or impacting of the mating fracture surfaces, or a combination of the two, and makes a quantitative interpretation of their significance somewhat uncertain. However, an estimate of the number of fine striations in the area illustrated in Figure 19, that was based on spacing measurements of a few well-defined lines, suggested a count of some 90 lines. Assuming a one to one correspondence between wheel rotation and fine striation formation, and based on an outside tire diameter of 44 in., an estimated roll distance of 1000 ft. was covered by the aircraft during the fatigue crack growth defined by this band of striations.

More clearly defined fracture surface topography in the form of fatigue striations and ductile dimples is illustrated in the micrograph, Figure 20, taken from a failed type "B" wheel. If the wheel rotation-striation correspondence is assumed, the count of 43 striations in this micrograph would represent an aircraft roll distance of some 500 ft. Neither this distance nor that previously estimated for the type "C" wheel would account for the estimated 5 roll miles for a typical landing cycle of a jet transport. Therefore manoeuvers such as pivoting, and brake application at high speed must be examined in an attempt to account for the relatively small number of fine fatigue striations on any one area of the various wheel fracture surfaces. Without correlative strain measurements under service conditions, no rational deductions can be made with respect to the pivoting manoeuvres.

The landing cycle described previously indicates a "2 second" brake application shortly after touchdown in order to reduce the aircraft speed from 180 to 100 miles per hour. If an average speed of 150 mph is assumed for the 2 second brake application, the distance travelled by the aircraft would have been of the order of 450 ft., which corresponds fairly closely to the roll distance estimated from the 43 fatigue striations. Thus, a cyclic stress condition in the wheel, favorable to crack growth by the mechanism of striation formation due to wheel rotation during brake application appears to be a plausible explanation for the limited number of striations observed in a given area of fracture surface. Figure 21 illustrates a second striated area on the fracture surface of a type "B" wheel, with some 60 striations visible. The fluctuation in striation spacing, corresponding to Figures 20 and 21, and, illustrated graphically in Figure 22, also reflects a gradual increase in striation spacing with time, which suggests a build-up in cyclic stress levels in the wheel hub as the application of brakes continues. Further credibility is given to the suggestion that braking does

in fact induce significant localized stresses in the wheel hubs. In Figure 23, in which fatigue crack nucleation in two types of wheels in an area adjacent to the brake rotor drive-blocks is illustrated.

The abundance of ductile dimples observed on the fracture surfaces of the type "B" wheels, even within a few millimeters of the crack origin, indicates zones of rapid fracture, likely due, in part, to high stress levels associated with landing impact loads.

3.3 Quantitative Crack Propagation Analysis of Aircraft Wheels

Crack propagation histories in terms of crack length and number of landings were determined for three different types of aluminum alloy main landing gear aircraft wheel hubs.

3.3.1 Type "A" Wheel

The 51.0 mm. crack in the bead seat radius of the type "A" wheel, Figure 9, which had penetrated the hub to a maximum depth of 9.0 mm. had been detected by means of ultra-sonic detection apparatus, so that catastrophic failure of the wheel was prevented. The total service time of the component was reported to be 8253 hours, and 2977 hours had elapsed since the previous ultra-sonic check.

Replicas of the fracture surface were analyzed with the aid of both light and electron microscopes. In terms of crack propagation information, the traverse of the first 0.4 mm. of crack penetration yielded no meaningful fracture surface details. The first indication of crack growth lines of the type illustrated in Figure 18, appeared some 0.45 mm. from the point of crack initiation. The method of determining the fatigue crack growth history consisted essentially of measuring the spacings of the crack growth lines, or where possible, of making direct line counts over discrete crack length intervals.

On the assumption that the line spacings represent the crack growth in the wheel during one landing cycle, and that

the average flight time of this aircraft in service is approximately one hour, the fatigue crack penetration during the final 1,064 landings was of the order of 8.8 mm. This radial crack penetration into the rim corresponded to an overall circumferential crack length of some 51 mm. The microscopic line count derivation for the wheel is listed in Table I, and the plot of the estimated number of landings against fatigue crack length is illustrated in Figure 24. From this information it was deduced that at a total service time of some 7,190 hours, the crack would have penetrated the hub to a depth of 0.5 mm. The total circumferential crack length, as derived from the semi-circular initiation area, Figure 11, would have been of the order of 1.0 mm. and it would seem improbable that such a small crack would have been detected, either by visual or ultra-sonic means.

3.3.2 Type "B" Wheels

For purposes of crack growth rate comparison, two catastrophically failed wheels of this type were fractographically analyzed.

Wheel Hub Type "B" - No.1

The point of crack initiation in this wheel was apparently located in the small discoloured semi-circular area shown in Figure 13. Although there was evidence of corrosion on the fracture surface, a distinct corrosion pit was not visible. When the crack had completely penetrated the rim in the radial direction, at a half-crack length of 22 mm., fatigue crack growth tended more towards the circumferential direction, and line spacings on the outer and inner sides of the rim became approximately equal. Once total penetration of the hub had occurred, the rate of crack growth increased rapidly, probably because of a significant increase in net section stress. This rapid increase in crack growth rate is reflected by the rapidly increasing slope of the curve, Figure 25, which correlates half-crack length with the number of landings.

A total of some 405 landings were accounted for over the fatigue crack interval 0.5 to 62 mm. Available information suggests that tire changes on this type of wheel are made on the average of every 125 landings. On this basis, it is estimated that the full length of the fatigue crack in the bead-seat radius at the time of the final tire change prior to wheel failure, would have been of the order of 25 to 28 mm.

Wheel Hub Type "B" - No.2

The point of fatigue crack initiation in this wheel hub, illustrated in Figure 26, appeared to be a corrosion pit on the outer surface of the rim. The circumferential crack penetrated the hub at a distance of approximately 40 mm. from the bead seat radius. As illustrated by the corresponding pairs of macroscopic growth lines (A,B, Figure 26), the rates of fatigue crack growth differed on either side of the crack origin. The final fatigue crack length on side A was 72 mm., and 58 mm. on side B, when catastrophic failure of the wheel occurred. A total of some 552 landings were accounted for over the half-crack length interval 2 mm. to 72 mm. It is of interest to note that notwithstanding the fact that this fatigue crack developed some 40 mm. in from the bead-seat radius, the change in the rate of fatigue crack growth as illustrated in Figure 27, is essentially identical to that determined for the previous type "B" wheel hub, Figure 25 which failed in the bead-seat radius.

3.3.3 Type "C" Wheel

Fatigue crack growth information for this wheel was determined over the 76 mm. crack interval identified in Figure 15. Although the crack was initiated at a point adjacent to the bead-seat radius, crack growth occurred primarily at an angle of some 60° to the wheel radius, through the wheel flange.

The graph, illustrated in Figure 28, accounts for some 903 landings over the fatigue crack interval 4 to 76 mm. The curve exhibited an approximately constant growth rate of 47 microns

per landing, over the range 4 to 40 mm. Over the crack interval 40 to 76 mm. the crack growth rate exhibited an abrupt increase to some 650 microns per landing. This latter interval corresponded to a clearly defined change in fracture surface topography (Figure 15) that exhibited a considerably coarser texture than the initial 40 mm. of fatigue crack length.

4.0 CONCLUDING REMARKS

The nature of the macroscopic growth lines on the fracture surfaces of the failed aircraft wheels (Figure 16), and the abundant evidence of the rapid fracture mode in the form of ductile dimples (Figure 20) suggest that landing impact stresses have played a significant role in crack growth in the various wheels. The limited number of microscopic fatigue striations observed on any one area of the fracture surfaces (Figure 20) indicates that fatigue damage resulting from the five roll miles per aircraft landing cycle may contribute less to wheel fatigue damage than the application of the brakes at high speed. It is clear that these parameters, among others are not adequately catered for in the conventional "Roll Test" qualification requirements for aircraft wheels.

The formulation of appropriate fatigue qualification tests for aircraft wheels would seem to require accurate information concerning the magnitudes of dynamic service stresses in the critical regions of the wheels. Such information could also be useful in the interpretation of the macroscopic crack growth lines on the fracture surfaces of the failed wheels, in terms of their microscopic content. In this way it might not only be possible for example, to determine the reasons for the variation in macroscopic line spacings (Figure 17), but fracture surface topography such as the fine fatigue striations (Figures 20 and 21) that have been attributed to high speed brake application could conceivably be specifically related to the cyclic operation

of the anti-skid device during brake application.

The correlation of the macroscopic growth lines on the fatigue fracture surfaces of laboratory specimens with the cyclic load spectra to which the specimens were subjected is relatively straightforward. This is not always so in the case of service failures in the absence of correlative strain measurements or some other dependable form of loading history for the component, so that assumptions must be made when interpreting the significance of the lines. Such assumptions appear to be justified in the case of the aircraft wheels, where the fairly regular spacings of the majority of the lines over long crack segments strongly suggest repeated loading sequences appropriate to aircraft landing cycles. In addition, the curves illustrating crack growth histories of the various wheels indicate reasonable values in terms of actual service history, and in general the plots are fairly smooth. Abrupt changes in the slope of a curve, such as that shown in Figure 28, can usually be correlated with abrupt changes in fracture surface topography, which in turn correspond to changes in dynamic stress levels in the wheel hub due to the decreases in component net section that result from increases in crack length.

5.0 ACKNOWLEDGEMENTS

The author wishes to thank Mr. J. A. Dunsby of this laboratory for supplying fatigue specimens fractured in the laboratory, and Mr. E. C. Bell and Mr. J. Reeves of Air Canada for supplying service failure specimens and for valuable discussions.

6.0 REFERENCES

(1) Final Minutes - 1969 Commercial Wheel and Brake Forum, Bendix Energy Controls Division, South Bend, Indiana, U.S.A., Sept. 1969, p.44.

(2) Aerospace Standard AS 227 D "Wheels and Brakes - Minimum Requirements for Civil Aircraft

Applications", Society of Automotive Engineers, 485 Lexington Ave., New York, Revised 15 April, 1963.

(3) Behr, R. D. Campbell, S. Roll Fatigue Tests on Forged ZK60A-T5 Magnesium and 2014-T6 Aluminum Wheels. Paper presented at Fifth Pacific Area Meeting, ASTM, Seattle Washington, 31 Oct. to 5 Nov. 1965.

(4) Military Specification MIL-W-5013G, Wheel and Brake Assemblies; Aircraft. 20 February, 1967.

(5) Landing Gear Ancillary Equipment - A Survey of Aircraft Tyres, Wheels, Brakes and the Research Facilities of the Dunlop Co. Ltd. Aircraft Engineering, Vol. XL, No.1, January 1968, P.9.

(6) Wiebe, W. Quantitative Fatigue Crack Propagation Analysis by Means of Electron Fractography. Report LR-450, National Aeronautical Establishment, National Research Council of Canada, March 1966.

(7) McMillan, J.C. Hertzberg, R.W. Application of Electron Fractography to Fatigue Studies. Electron Fractography, ASTM STP 436, American Society for Testing and Materials, 1968, pp.89-123.

(8) Forsyth, P.J.E. The Physical Basis of Metal Fatigue. Blackie and Son Ltd., London and Glasgow, 1969, p.67.

TABLE I

LINE COUNT DERIVATION - TYPE "A" WHEEL

Crack Length Interval (mm.)	Interval Width (mm.)	Average Line Spacing (microns)	Interpolated Line Count
1.0 to 2.3	1.3	23.6	55
2.3 to 5.0	2.7	18.9	143
5.0 to 5.8	0.8	25.2	32
5.8 to 6.3	0.5	13.2	38
6.3 to 7.2	0.9	22.3	40
7.2 to 7.7	0.5	14.0	36
7.7 to 8.5	0.8	24.9	32
8.5 to 11.0	2.5	26.0	96
11.0 to 12.0	1.0	30.4	33
12.0 to 14.4	2.4	46.1	52
14.4 to 16.0	1.6	61.4	26
16.0 to 18.2	2.2	64.2	34
18.2 to 20.2	2.0	60.8	33
20.2 to 22.0	1.8	75.2	24
22.0 to 24.0	2.0	80.3	25
24.0 to 26.5	2.5	81.0	31
26.5 to 28.8	2.3	70.1	33
28.8 to 31.0	2.2	70.3	31
31.0 to 33.0	2.0	63.0	32
33.0 to 35.5	2.5	76.2	33
35.5 to 45.0	9.5	75.7	126
45.0 to 46.5	1.5	71.3	21
46.5 to 49.0	2.5	75.1	33
49.0 to 51.0	2.0	79.0	25
		Total	1,064

X 3

FIG. 1(a) BANDED STRUCTURE ON FRACTURE SURFACES OF A LABORATORY SPECIMEN SUBJECTED TO REPETITIVE SEQUENTIAL LOADING

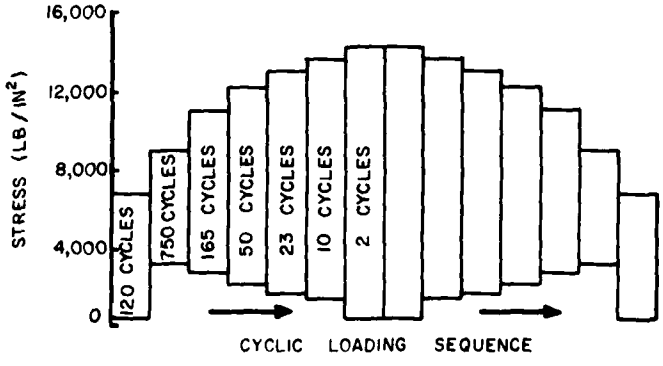

FIG. 1(b) CYCLIC LOADING SEQUENCE OF WING LOAD SPECTRUM

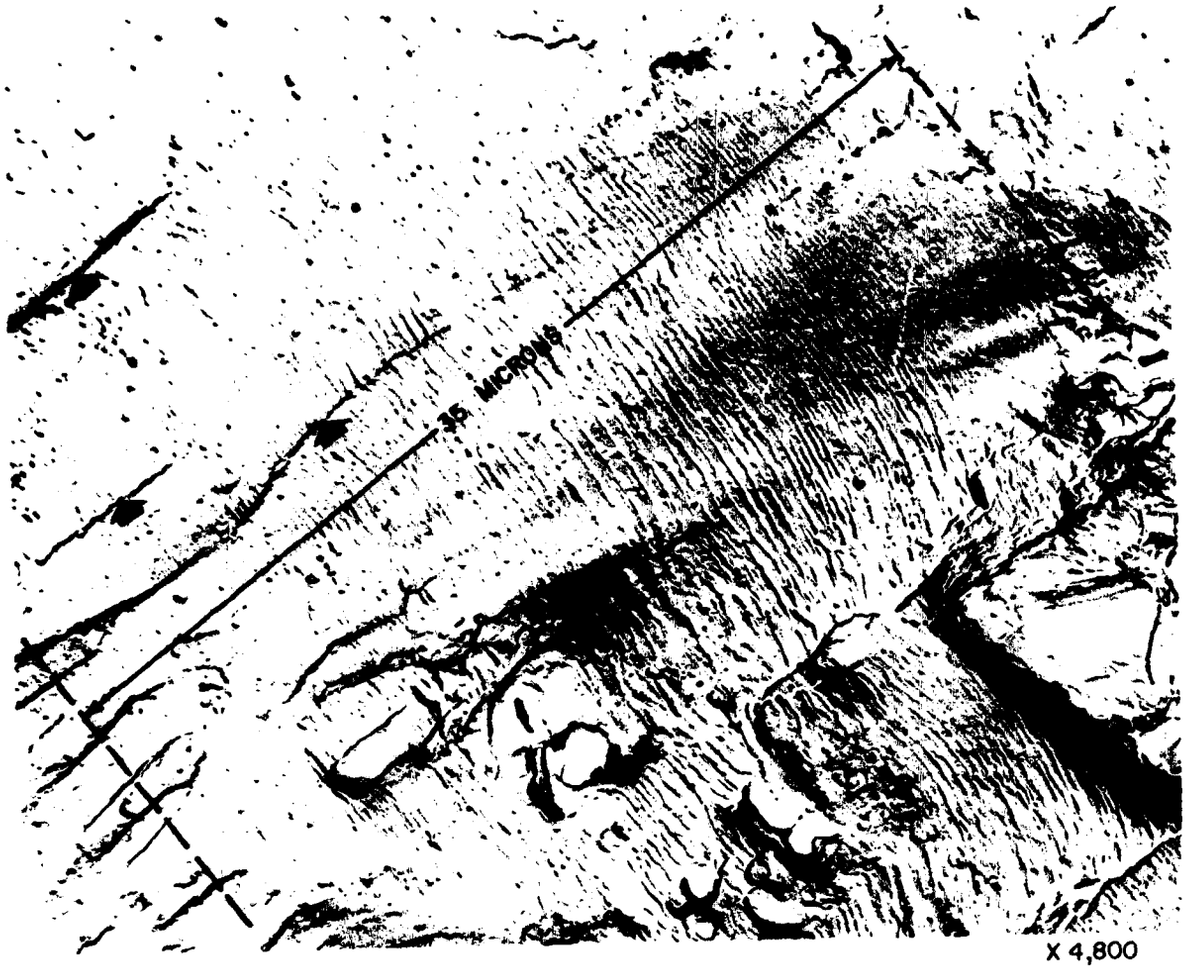

FIG. 2 ELECTRON MICROGRAPH OF THE FRACTURE SURFACE TOPOGRAPHY OF ONE MACROSCOPIC BAND

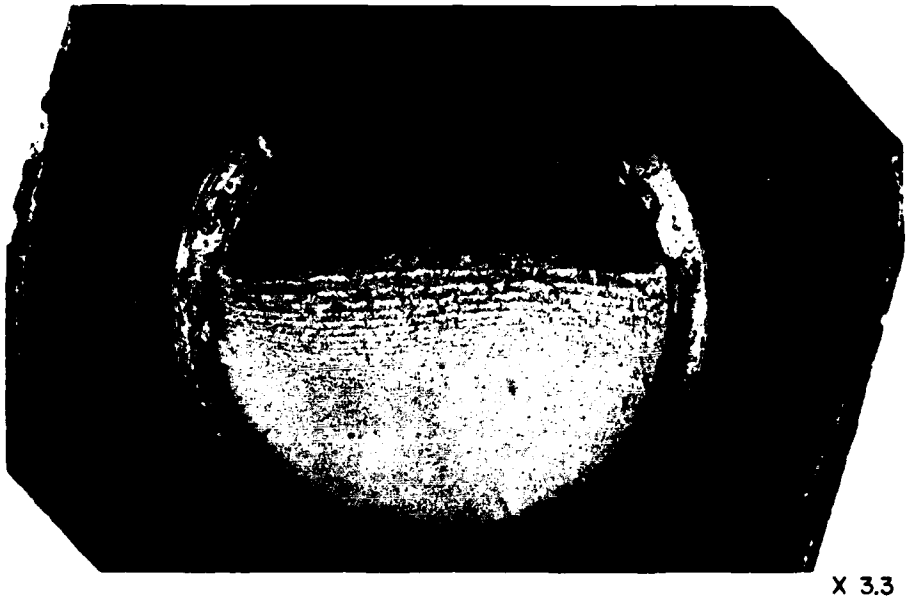

X 3.3

FIG. 3(a) FRACTURE SURFACE OF A STEEL BOLT SUBJECTED TO REPETITIVE SEQUENTIAL LOADING

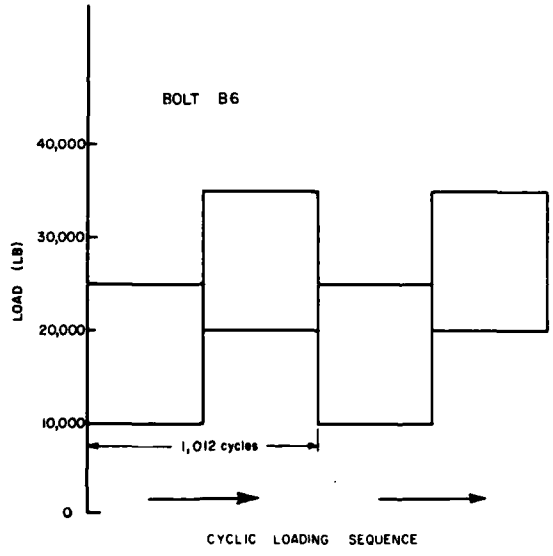

FIG. 3(b) REPITITIVE LOADING SEQUENCE APPLIED TO STEEL BOLT

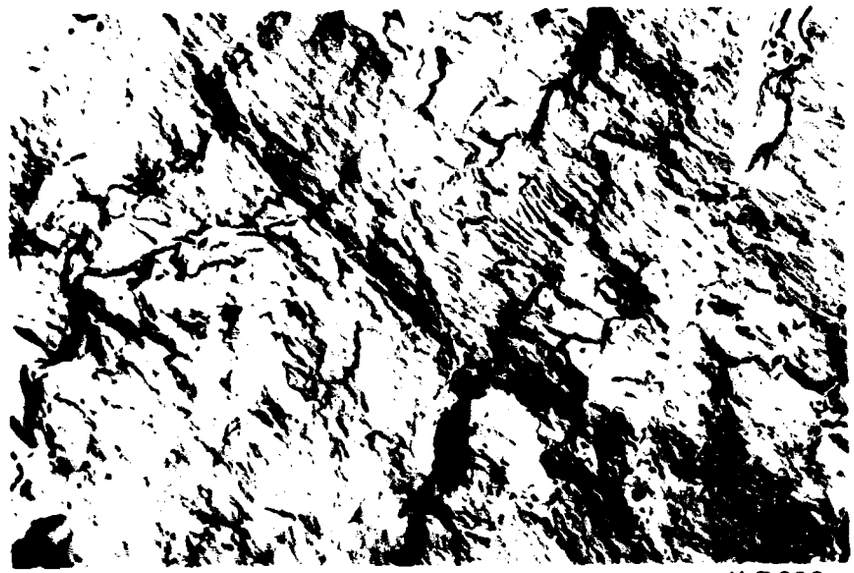

X 7,000

FIG. 4 FATIGUE STRIATIONS ON BRIGHT BANDS OF STEEL BOLT FRACTURE SURFACE

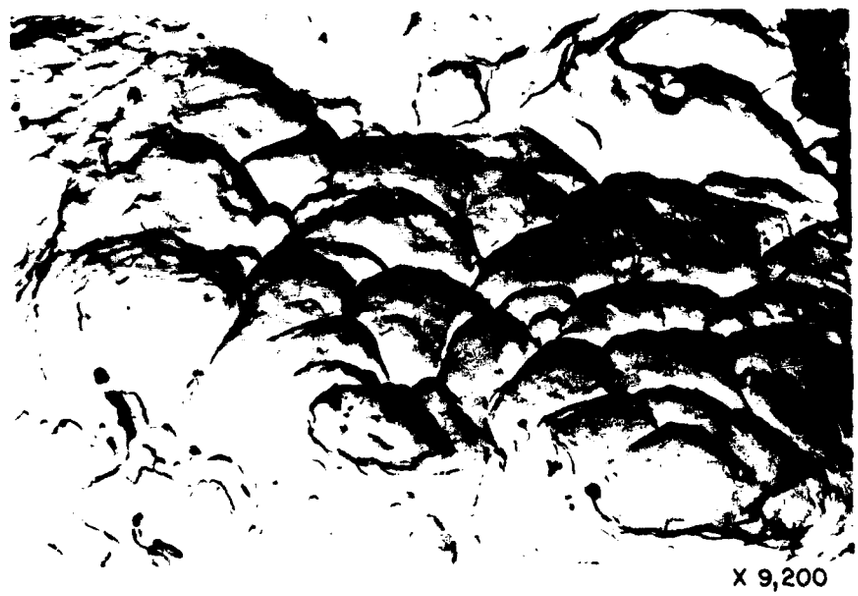

X 9,200

FIG. 5 MICROVOID COALESCENCE ON DULL BANDS OF STEEL BOLT FRACTURE SURFACE

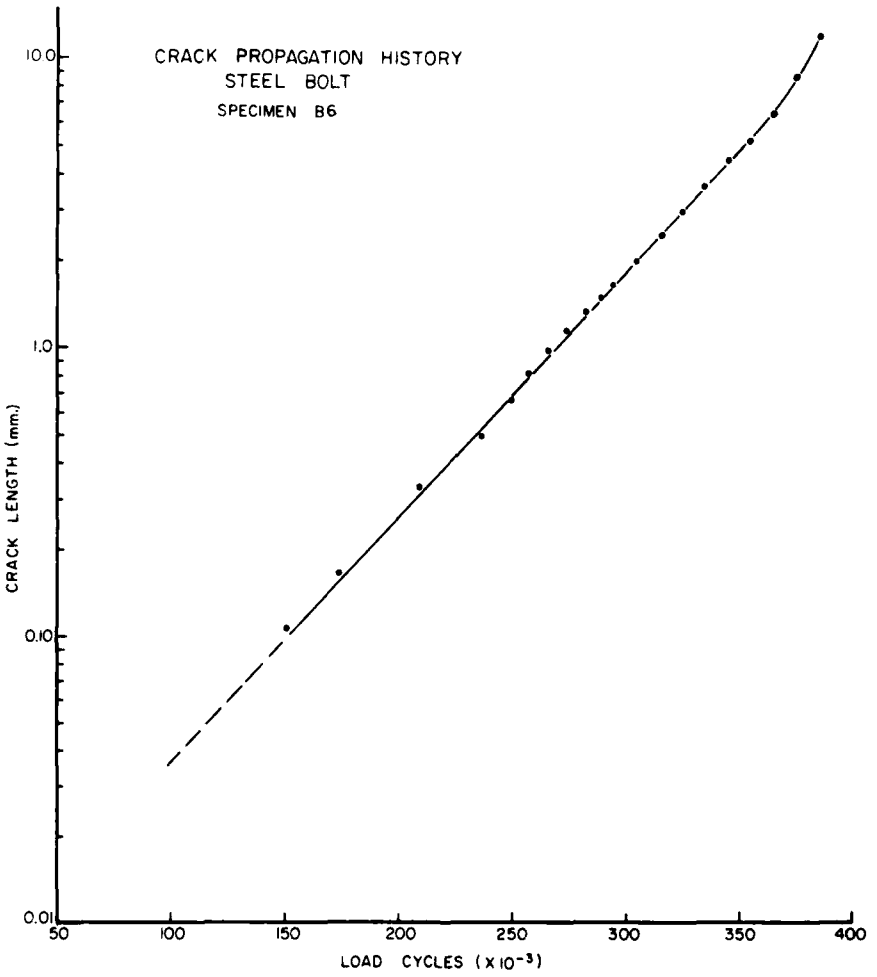

FIG. 6 CRACK PROPAGATION HISTORY – STEEL BOLT

X70

FIG. 7(a) REGULARLY SPACED BANDS ON FRACTURE SURFACE OF SPAR CAP IN LABORATORY FATIGUE TEST

X 30

FIG. 7(b) RANDOMLY SPACED LINES ON FATIGUE FRACTURE SURFACE OF SPAR CAP CRACK FORMED IN SERVICE

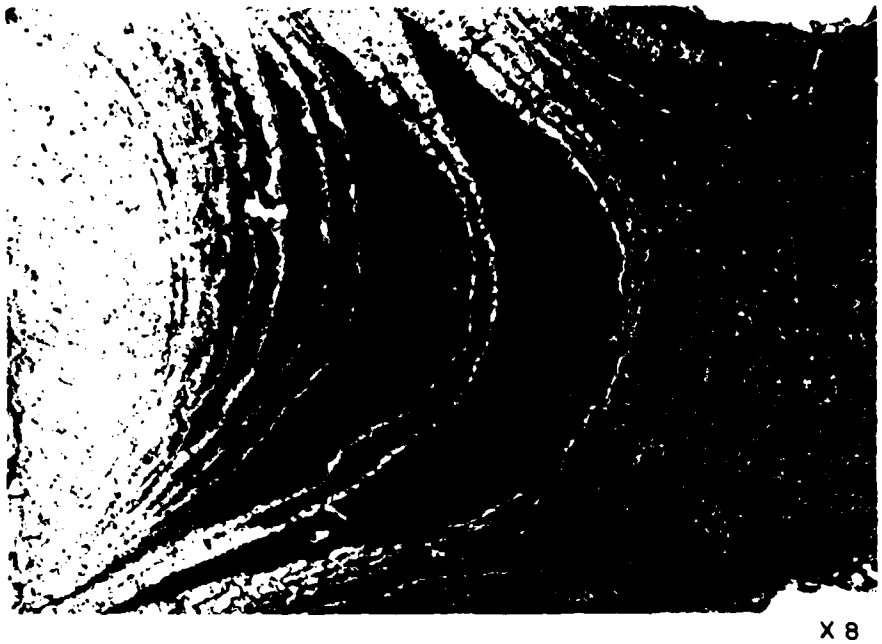

X 8

FIG. 8(a) TRANSMITTED LIGHT REPLICA MACROGRAPH OF THE FRACTURE SURFACE OF FAILED ROTOR-BLADE TINE

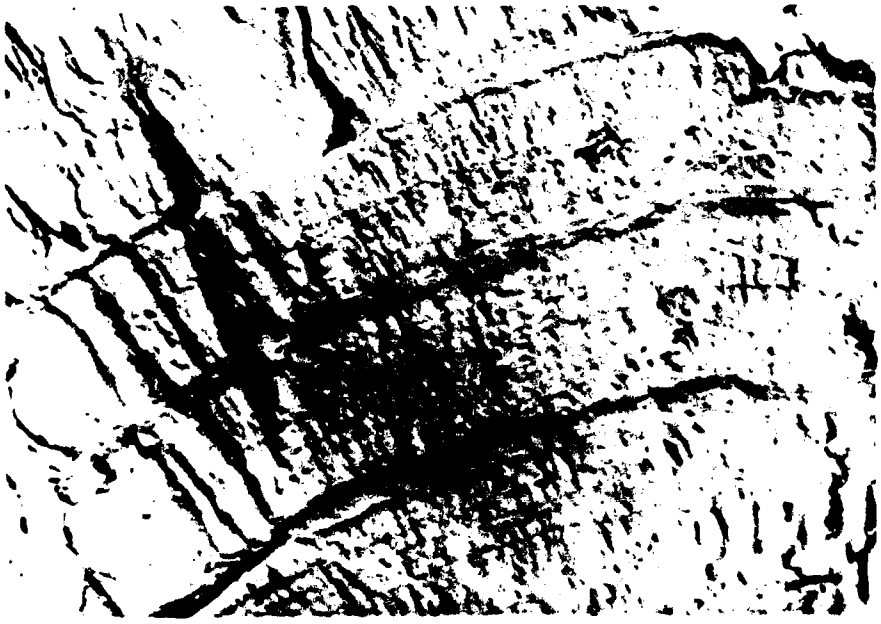

X 9,800

FIG. 8(b) MICROSCOPIC FATIGUE STRIATIONS ON BRIGHT BANDS OF ROTOR-BLADE TINE

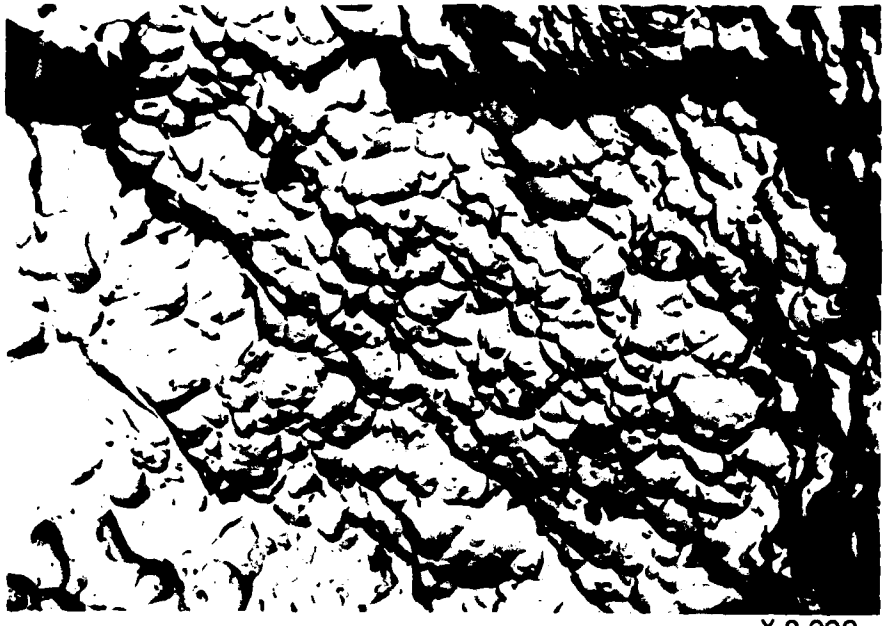

X 9,000

FIG. 8(c) MICROVOID COALESCENCE ON DULL BANDS OF ROTOR-BLADE TINE

X 4

FIG. 9 FATIGUE FRACTURE SURFACE – WHEEL TYPE "A"
(ARROW INDICATES CORROSION PIT)

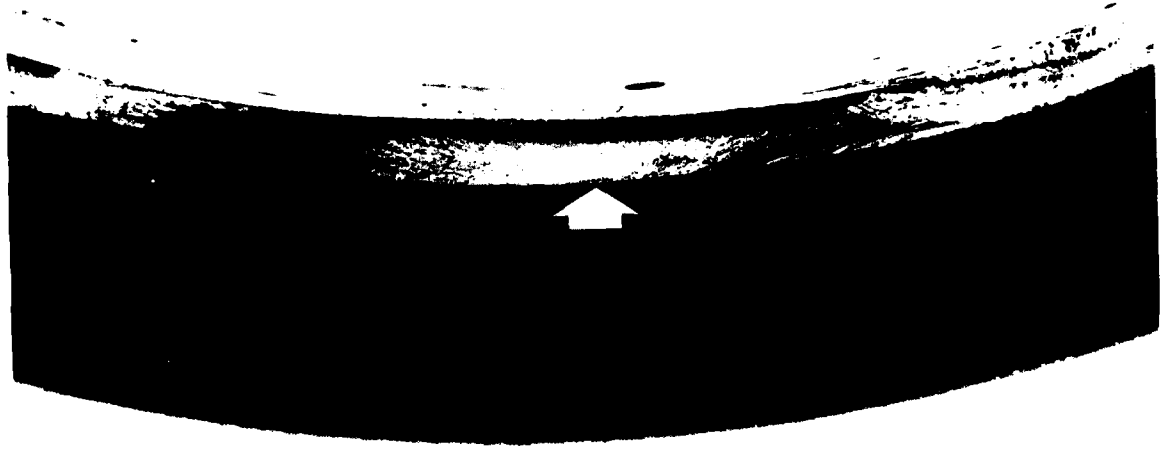

X 1.2

FIG. 10 FATIGUE FRACTURE SURFACE - WHEEL TYPE "B"
(ARROW INDICATES CORROSION PIT)

X 75

FIG. 11 ENLARGED VIEW OF CORROSION PIT, AND INITIAL FATIGUE FRACTURE SURFACE AREA- WHEEL TYPE "A"

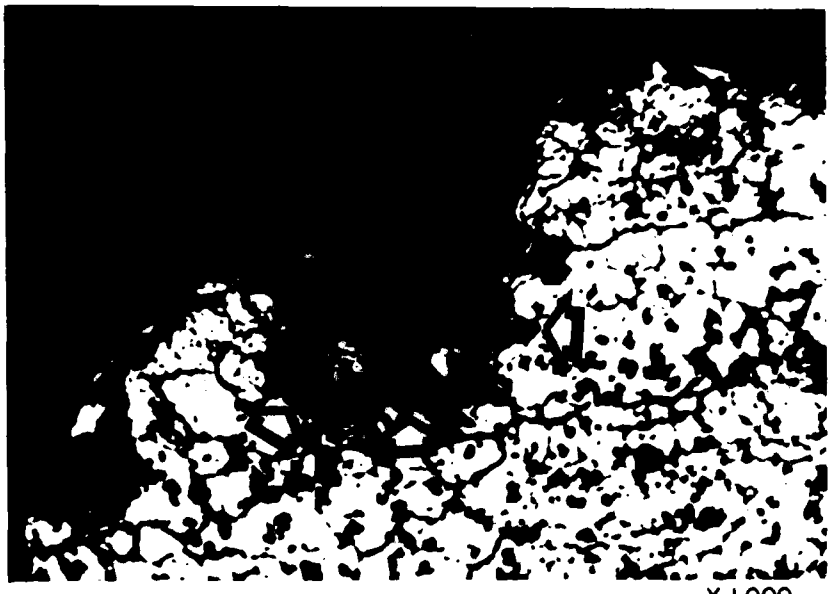

X 1,000

FIG. 12 METALLOGRAPHIC SECTION THROUGH CORROSION PIT - WHEEL TYPE "A"

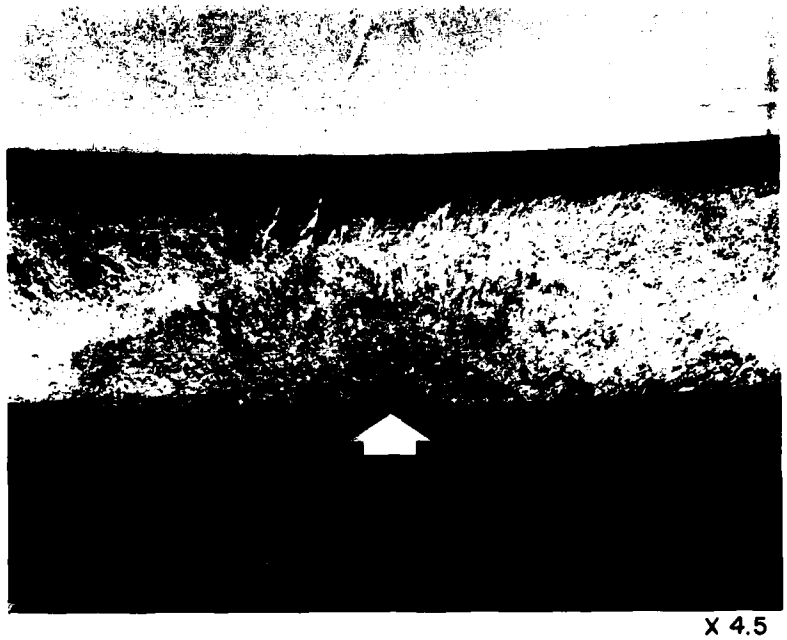

X 4.5

FIG. 13 SEMI-CIRCULAR AREA EXHIBITING CORROSION IN THE INITIATION REGION OF FATIGUE CRACK – WHEEL TYPE "B"

X 2.8

FIG. 14 MULTIPLE FATIGUE CRACKS NUCLEATED AT CORROSION PITS IN BEAD-SEAT RADIUS OF AN AIRCRAFT WHEEL

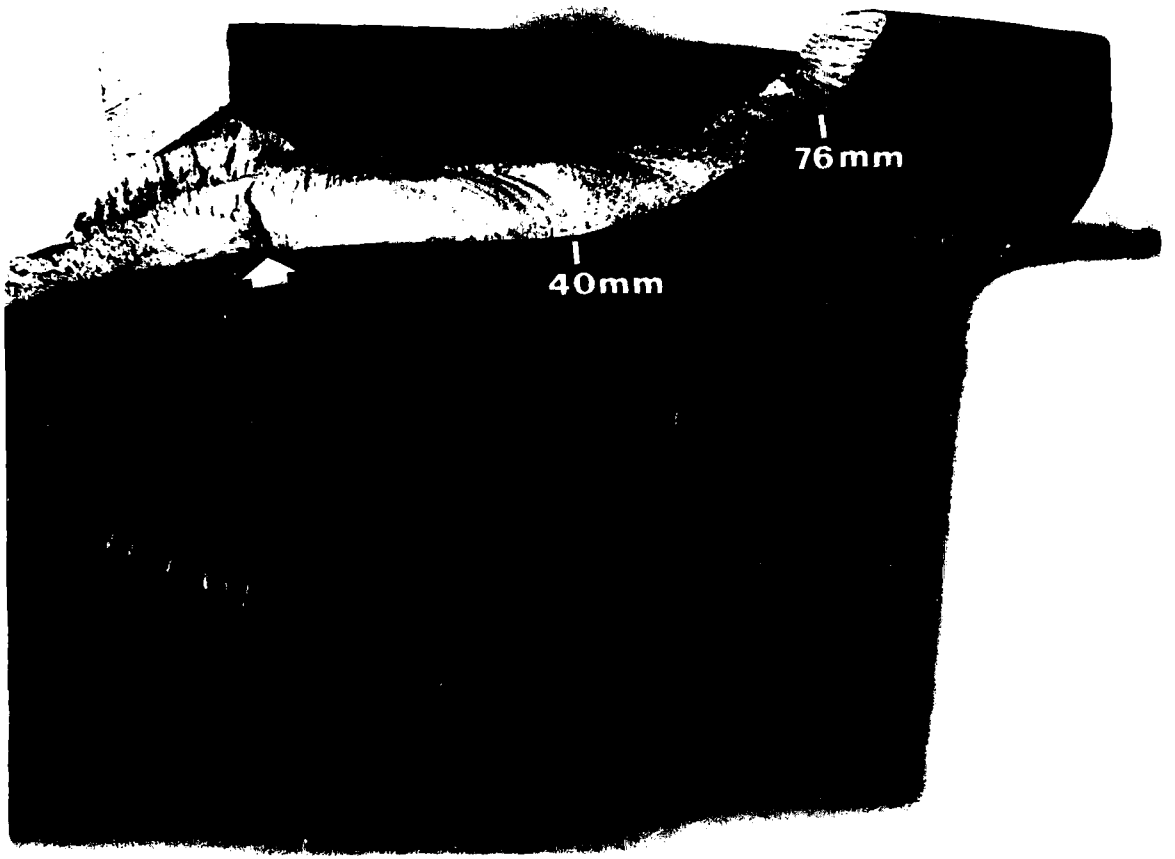

X 1.1

FIG. 15 FATIGUE FRACTURE SURFACE - WHEEL TYPE "C"
(ARROW INDICATES REGION OF CRACK NUCLEATION)

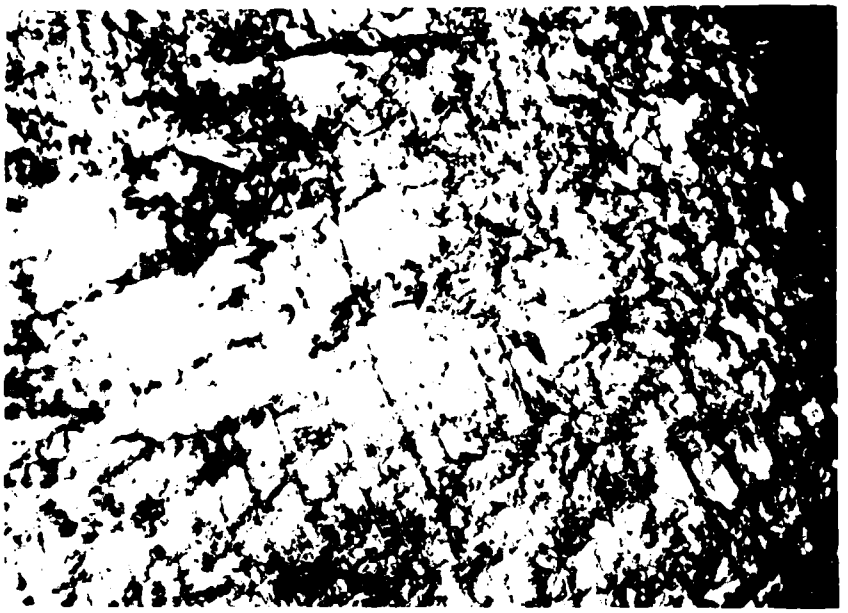

X 130

FIG. 16 CRACK PROGRESSION LINES - WHEEL TYPE "C"

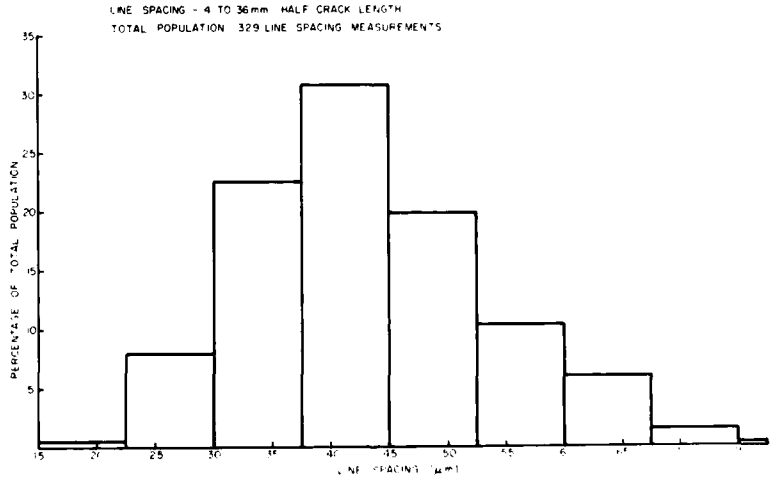

FIG. 17 LINE SPACING DISTRIBUTION - WHEEL TYPE "C"

X 3,500

FIG. 18 MICROSCOPIC BANDS IN EARLY STAGES OF CRACK GROWTH -WHEEL TYPE "A"
(ARROW INDICATES DIRECTION OF CRACK GROWTH)

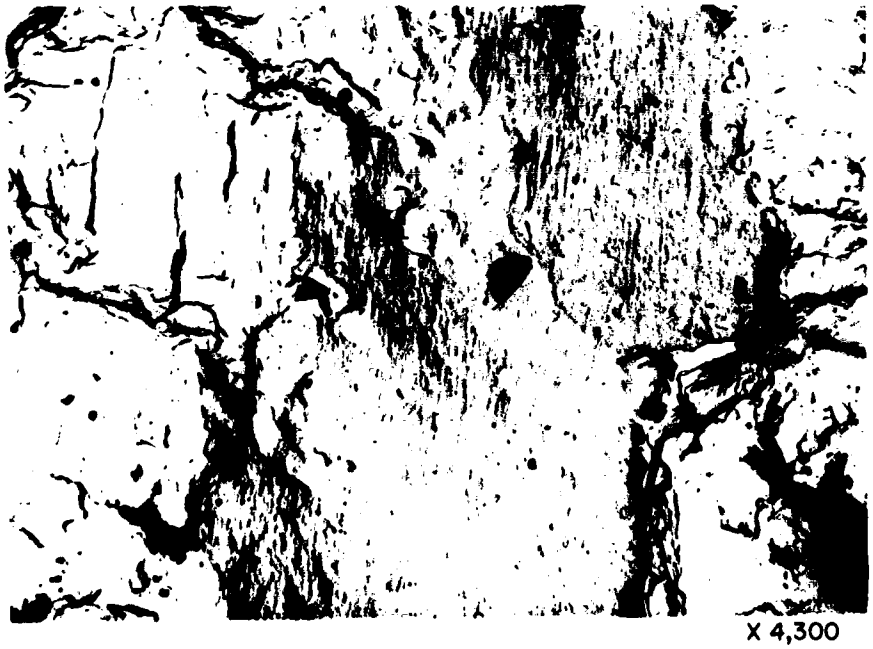

X 4,300

FIG. 19 MICROSCOPIC FRACTURE SURFACE TOPOGRAPHY – WHEEL TYPE "C"

X 7,200

FIG. 20 MICROSCOPIC FATIGUE STRIATIONS AND DUCTILE DIMPLES
WHEEL TYPE "B"

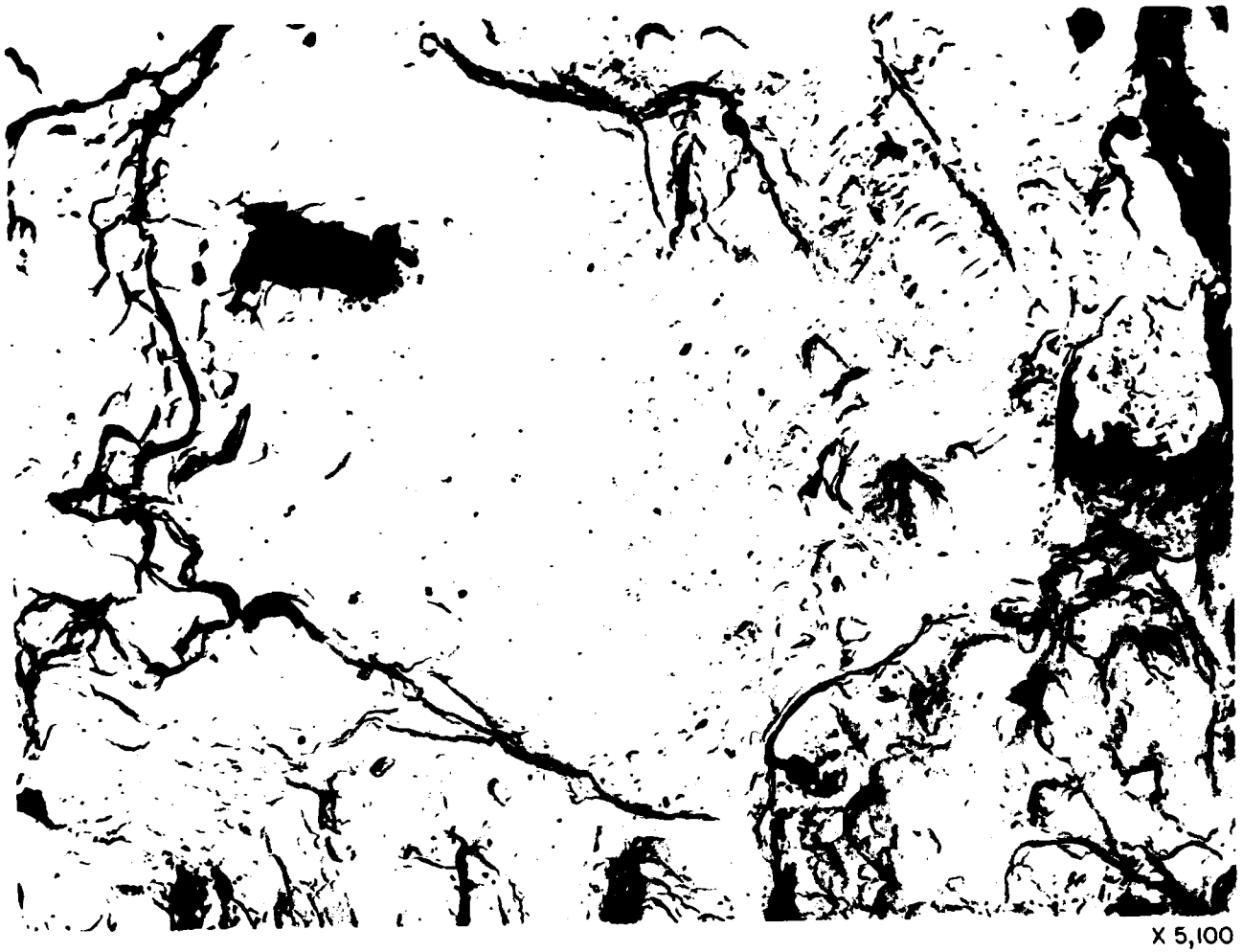

X 5,100

FIG. 21 STRIATED AREA ON FRACTURE SURFACE OF WHEEL TYPE "B"

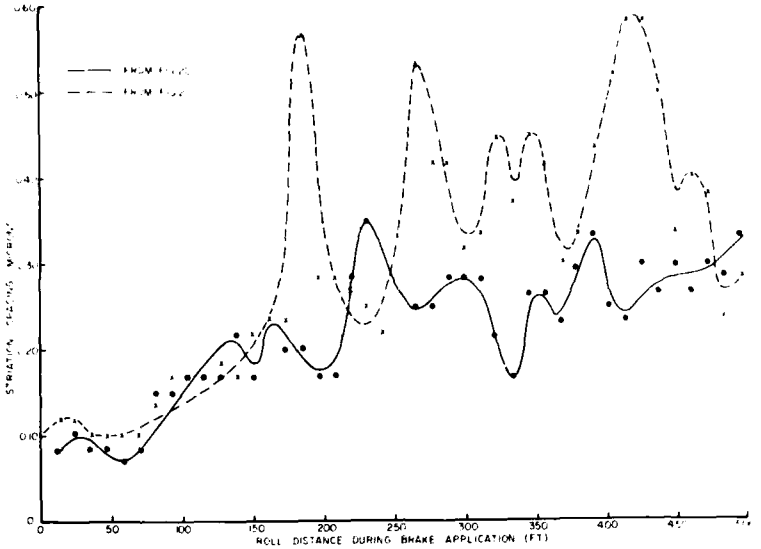

FIG. 22 FLUCTUATION IN MICROSCOPIC STRIATION SPACING ON FRACTURE SURFACE OF WHEEL TYPE "B"

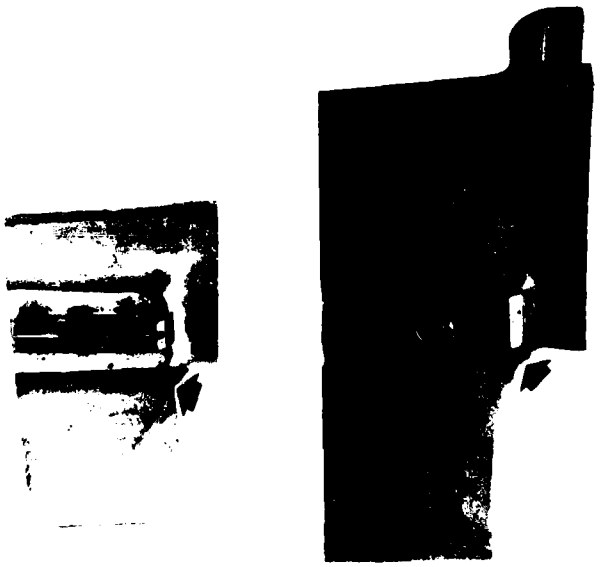

FIG. 23 FATIGUE CRACK NUCLEATION ADJACENT TO BRAKE ROTOR DRIVE-BLOCKS

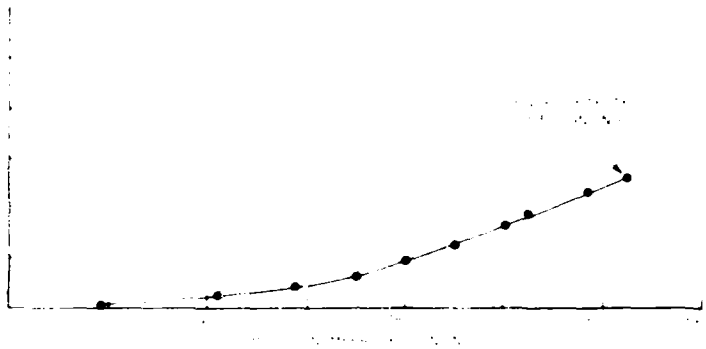

FIG 24 CRACK GROWTH HISTORY - WHEEL TYPE "A"

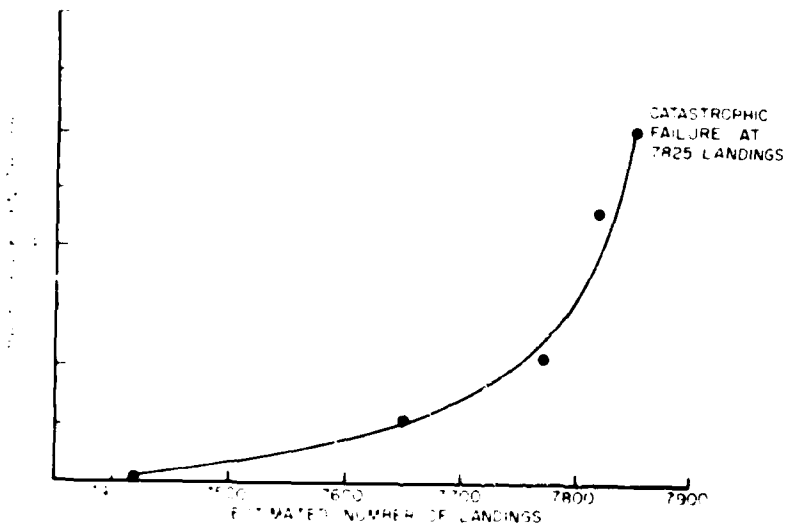

FIG 25 CRACK GROWTH HISTORY - WHEEL TYPE "B", No. 1

FIG. 26 FATIGUE FRACTURE SURFACE - WHEEL TYPE "B", No. 2
(ARROW INDICATES POINT OF CRACK NUCLEATION)

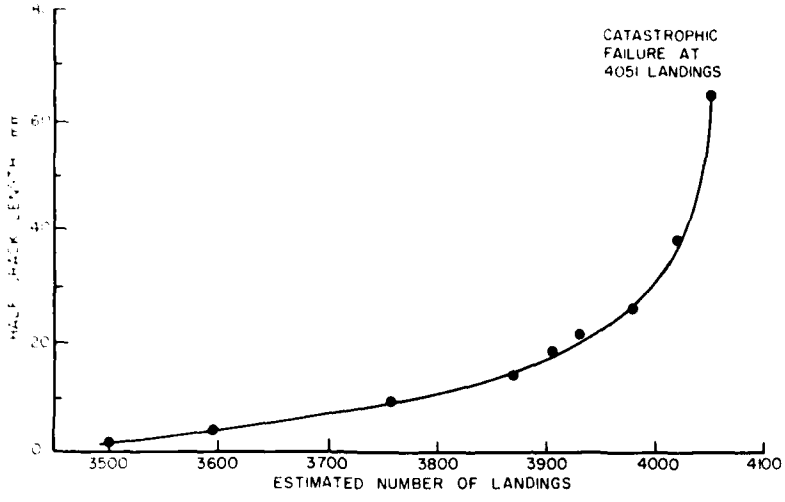

FIG. 27 CRACK GROWTH HISTORY - WHEEL TYPE "B", No. 2

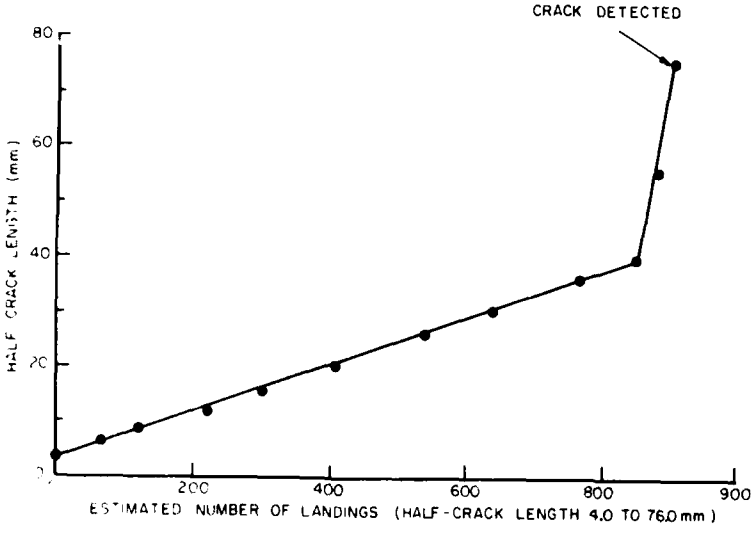

FIG. 28 CRACK GROWTH HISTORY - WHEEL TYPE "C"